



Brassinosteroids mitigate iron deficiency improving nutritional status and photochemical efficiency in *Eucalyptus urophylla* plants

Michael Douglas Roque Lima¹ · Udson de Oliveira Barros Junior¹ · Bruno Lemos Batista² · Allan Klynger da Silva Lobato¹

Received: 29 March 2018 / Accepted: 25 June 2018 / Published online: 25 July 2018
© Springer-Verlag GmbH Germany, part of Springer Nature 2018

Abstract

Iron (Fe) is essential for the biosynthesis of constitutive proteins of chloroplasts, mitochondria and other organelles, and its deficiency triggers negative effects on photochemical efficiency and electron transport. Brassinosteroids are steroids that play beneficial roles related to chlorophyll fluorescence and plant nutrition. The aims of this research were to answer if epibrassinolide (EBR) can mitigate Fe deficiency in *Eucalyptus urophylla* plants and to evaluate the repercussions on nutritional status and physiological and biochemical behaviours. The experiment followed a completely randomized factorial design with two Fe conditions (Fe deficiency and control) and three levels of 24-epibrassinolide (0, 50 and 100 nM EBR). EBR application in *E. urophylla* plants exposed to Fe deficiency increased Fe contents in root, stem and leaf. EBR reduced the negative effects of Fe deficiency on chlorophyll fluorescence and gas exchange parameters. Fe deficiency caused reductions in Chl *a*, Chl *b* and total Chl, while plants sprayed with 100 nM EBR showed significant increases in these variables. Our results clearly reveal that EBR attenuated the negative effects caused by Fe deficiency on nutritional status and in the physiological and biochemical behaviours of *E. urophylla* plants, and these results were connected to increases in the contents of macronutrients and micronutrients, including Fe. EBR also improved the photochemical efficiency of PSII, gas exchange and photosynthetic pigments, inducing minor accumulations of oxidative compounds. Additionally, *E. urophylla* plants submitted to 100 nM of EBR had better nutritional, biochemical, physiological and morphological results.

Keywords 24-Epibrassinolide · Chloroplast · Fe supply · Micronutrient · Photosystem II

Abbreviations

Φ_{PSII}	Effective quantum yield of PSII photochemistry
BRs	Brassinosteroids
CAR	Carotenoids
Chl <i>a</i>	Chlorophyll <i>a</i>
Chl <i>b</i>	Chlorophyll <i>b</i>
C_i	Intercellular CO ₂ concentration
CO ₂	Carbon dioxide
Cyt- <i>b₆/f</i>	Cytochrome <i>b₆/f</i> complex

<i>E</i>	Transpiration rate
EBR	Epibrassinosteroids
EL	Electrolyte leakage
ETR	Electron transport rate
ETR/ P_N	Ratio between the apparent electron transport rate and net photosynthetic rate
EXC	Relative energy excess at the PSII level
Fd	Ferredoxin
Fe	Iron
F_m	Maximal fluorescence yield of the dark-adapted state
F_0	Minimal fluorescence yield of the dark-adapted state
F_v	Variable fluorescence
F_v/F_m	Maximal quantum yield of PSII photochemistry
g_s	Stomatal conductance
H ₂ O ₂	Hydrogen peroxide
LDM	Leaf dry matter
MDA	Malondialdehyde

Communicated by Wieser.

✉ Allan Klynger da Silva Lobato
allanlobato@yahoo.com.br

¹ Núcleo de Pesquisa Vegetal Básica e Aplicada, Universidade Federal Rural da Amazônia, Rodovia PA 256, Paragominas, Pará, Brazil

² Centro de Ciências Naturais e Humanas, Universidade Federal do ABC, Santo André, São Paulo, Brazil

NPQ	Nonphotochemical quenching
O_2^-	Superoxide
P_N	Net photosynthetic rate
P_N/C_i	Instantaneous carboxylation efficiency
PSII	Photosystem II
q_P	Photochemical quenching
RDM	Root dry matter
ROS	Reactive oxygen species
RuBisCo	Ribulose-1,5-bisphosphate carboxylase/ oxygenase
SDM	Stem dry matter
TDM	Total dry matter
Total Chl	Total chlorophyll
WUE	Water-use efficiency

Introduction

The *Eucalyptus* genus is composed of several species that present rapid growth, broad adaptability and multiple utilizations of the wood, all characteristics that contribute to a reduction in pressure on native forests and associated biodiversity (Grattapaglia and Kirst 2008). In this context, areas planted with *Eucalyptus* are directed to the production of particleboard, charcoal, sawn wood and cellulose pulp, as well as non-wood products such as essential oils and honey (Gonçalves et al. 2008).

Areas with *Eucalyptus* have expanded in the world, covering a territory of approximately 20 million hectares (Mora et al. 2017). In Brazil, commercial *Eucalyptus* plantations covered an area of 5.7 million hectares in 2016, with an average productivity of 35.7 m³ ha⁻¹ per year, the best in global ranking among countries (IBA 2017).

Of all essential micronutrients, iron (Fe) is the most absorbed by plants (Baker et al. 2003). In soils, Fe is mainly found as insoluble polymers of iron oxide, such as Fe(OH)²⁺, Fe(OH)₃ and Fe(OH)₄⁻ produced from rock weathering (Guerinot and Yi 1994; Kraemer 2004; Tsai and Schmidt 2017). Despite the abundance of Fe in the soil, this element is generally not available to plants; during soil formation, Fe is released and transformed in insoluble forms (oxides and hydroxides) by oxidative hydrolytic reactions, conferring a reddish colour to soil rich in Fe (Schwertmann 1991; Guerinot 2001).

Fe is essential to plant development (Giehl et al. 2009), in which it participates in essential metabolic processes such as photosynthesis, respiration, nitrogen fixation, hormone synthesis and electron transfer (Sahrawat 2004; Layer et al. 2010). In addition, Fe acts on the composition of several compounds and enzymes, including catalase, peroxidase, cytochrome oxidase, leghemoglobin and ferredoxin (Hänsch and Mendel 2009; Eskandari 2011; Rout and Sahoo 2015; Krohling et al. 2016).

Fe absorption in *Eucalyptus urophylla* plants occurs due to the reduction of Fe³⁺ to Fe²⁺, a process regulated by the enzyme ferric chelate reductase (FCR) and rhizosphere acidification promoted by the proton extrusion via H⁺-ATPase, an enzyme that uses as substrate the hydrogen generated by H⁺-ATPase. After reduction, Fe²⁺ is transported by the iron-regulated transporter 1 (IRT1) from soil to the interior of the root cells (Yi and Guerinot 1996; Robinson et al. 1999; Vert et al. 2002).

Fe deficiency in plants often causes negative inferences on constitutive proteins of the chloroplasts, such as the cytochrome (*Cyt*) *b₆/f* complex and ferredoxin (Fd), decreasing the efficiencies of photosystem II and electron transport (Abadía et al. 1999; Morales et al. 2000; Roncel et al. 2016). The *Cyt-b₆/f* complex is responsible for the transference of electrons from PSII to PSI, generating an electrochemical gradient of protons in the membrane used during ATP synthesis (Kurisu et al. 2002). In addition, Fd is a protein composed of Fe and S (Fe–S protein) (Balk and Lobréaux 2005) responsible for donating electrons to the process of photosynthesis and the reduction of NADP⁺ to NADPH (Fromme et al. 2003; Ceccarelli et al. 2004; Merchant and Helmann 2012).

A possible solution to damages caused by Fe deficiency in plants can be the exogenous application of 24-epibrassinolide (EBR). EBR is the most bioactive form of brassinosteroids (BRs) (Bishop and Koncz 2002), which are substances classified as polyhydroxylated steroids (Clouse 2002). These steroids occur in the plant kingdom and play essential roles for growth and development, stimulating cell elongation and division (Clouse and Sasse 1998; Fujioka and Yokota 2003). The occurrences of BRs have been verified in several organs of plants, such as pollen, flowers, fruits, seeds, leaves, stems and roots (Bajguz and Hayat 2009).

In metabolism, BRs contribute positively to photochemical efficiency (Thussagunpanit et al. 2015), gas exchange (Swamy and Rao 2009), chlorophyll function (Yu et al. 2004), antioxidative metabolism (Xia et al. 2009) and plant growth (Abdullahi et al. 2003). In addition, BRs activate the proton pump, stimulate the synthesis of proteins and nucleic acids (Bajguz 2000) and modulate gene expression (Mussig et al. 2002).

Our hypothesis focused on the negative impacts caused by Fe deficiency on photochemical efficiency. We also investigated the benefits of EBR spray on plants, more specifically on the increase of Fe content in leaf tissue (Santos et al. 2018) and on the improvement in photosystem II function (Lima and Lobato 2017). Therefore, this research aimed to answer if EBR can mitigate Fe deficiency in *E. urophylla* plants, evaluating repercussions on nutritional status and physiological and biochemical behaviours.

Materials and methods

Location and growth conditions

The experiment was performed on the campus of Paragominas of the Universidade Federal Rural da Amazônia, Paragominas, Brazil (2°55'S, 47°34'W). The study was conducted in a greenhouse with temperature and humidity control. The minimum, maximum, and median temperatures were 20, 31 and 24.5 °C, respectively. The relative humidity during the experimental period varied between 60 and 80%.

Plants, containers and acclimation

Thirty-eight-day-old seedlings of *E. urophylla* S.T. Baker from DACKO™ presenting similar aspects and sizes were selected and placed in 1.2-L containers (0.15 m in height and 0.10 m in diameter) filled with substrate mix composed of sand and vermiculite in a 2:1 proportion. For semi-hydroponic cultivation, the previously described containers were equipped with one hole in the bottom covered with mesh, and solution absorption by capillary action, being misplaced into other containers (0.15 m in height and 0.15 m in diameter) containing 500 mL of nutritive Hoagland and Arnon (1950) solution adjusted to the nutritional exigencies of this species. The ionic force started at 50%, and it was modified to 100% after 2 days. After these periods, the nutritive solution remained with the total ionic force. Additionally, 40-day-old plants were submitted to Fe deficiency and control treatments.

Experimental design

The experiment followed a completely randomized factorial design with two Fe conditions (Fe deficiency and control) and three levels of 24-epibrassinolide (0, 50 and 100 nM EBR). With five replicates for each of six treatments, a total of 30 experimental units were used in the experiment, with one plant in each unit.

24-epibrassinolide (EBR) preparation and application

Forty-day-old seedlings were sprayed with 24-epibrassinolide (EBR) or Milli-Q water (containing a proportion of ethanol that was equal to that used to prepare the EBR solution) at 6-day intervals until day 76. The 0, 50 and 100 nM EBR (Sigma-Aldrich, USA) solutions were prepared by dissolving the solute in ethanol followed by dilution with

Milli-Q water [ethanol:water (v/v) = 1:10,000] (Ahmed et al. 2013).

Plant conduction and Fe deficiency treatment

One plant per pot was used to examine the plant parameters. The plants received the following macro- and micronutrients contained in the nutrient solution (Sigma-Aldrich, USA): 8.75 mM KNO₃, 7.5 mM Ca(NO₃)₂·4H₂O, 3.25 mM NH₄H₂PO₄, 1.5 mM MgSO₄·7 H₂O, 62.50 μM KCl, 31.25 μM H₃BO₃, 2.50 μM MnSO₄·H₂O, 2.50 μM ZnSO₄·7H₂O, 0.63 μM CuSO₄·5H₂O and 0.63 μM NaMoO₄·5H₂O, with Fe concentrations adjusted to each treatment. For Fe treatments, FeCl₂·4H₂O + EDTA was used at concentrations of 2.5 μM (Fe deficiency) and 250 μM (control) applied over 36 days (days 40–76 after the start of the experiment). During the study, the nutrient solutions were changed at 07:00 h at 3-day intervals, with the pH adjusted to 5.5 using HCl or NaOH. On day 76 of the experiment, physiological and morphological parameters were measured for all plants, and leaf tissues were harvested for biochemical and nutritional analyses.

Measurement of chlorophyll fluorescence

The minimal fluorescence yield of the dark-adapted state (F_0), maximal fluorescence yield of the dark-adapted state (F_m), variable fluorescence (F_v), maximal quantum yield of PSII photochemistry (F_v/F_m), effective quantum yield of PSII photochemistry (Φ_{PSII}), photochemical quenching coefficient (q_p), non-photochemical quenching (NPQ), electron transport rate (ETR), relative energy excess at the PSII level (EXC) and ratio between the electron transport rate and the net photosynthetic rate (ETR/ P_N) were determined using a modulated chlorophyll fluorometer (model OS5p, Opti-Sciences, USA). Chlorophyll fluorescence was measured in fully expanded leaves under light. Preliminary tests determined the location of the leaf, the part of the leaf and the time required to obtain the greatest F_v/F_m ratio; therefore, the acropetal third of leaves that were in the middle third of the plant and adapted to the dark for 30 min was used in the evaluation. The intensity and duration of the saturation light pulse were 7500 μmol m⁻² s⁻¹ and 0.7 s, respectively.

Evaluation of gas exchange

The net photosynthetic rate (P_N), transpiration rate (E), stomatal conductance (g_s), and intercellular CO₂ concentration (C_i) were evaluated using an infrared gas analyser (model LCPro⁺, ADC BioScientific, UK). These parameters were measured at the adaxial surface of fully expanded leaves that were collected from the middle region of the plant. The water-use efficiency (WUE) was estimated according to Ma

et al. (2004), and the instantaneous carboxylation efficiency (P_N/C_i). Gas exchange was evaluated in all plants under constant conditions of CO_2 concentration, photosynthetically active radiation, air-flow rate and temperature in a chamber at $360 \mu\text{mol mol}^{-1} \text{CO}_2$, $800 \mu\text{mol photons m}^{-2} \text{s}^{-1}$, $300 \mu\text{mol s}^{-1}$ and $28 \text{ }^\circ\text{C}$, respectively, between 10:00 and 12:00 h.

Extraction of superoxide

Superoxide was extracted from leaf tissue as per the method of Badawi et al. (2004). The extraction mixture was prepared by homogenizing 500 mg of fresh plant material in 5 mL of extraction buffer, consisting of 50 mM phosphate buffer (pH 7.6), 1.0 mM ascorbate and 1.0 mM EDTA. Samples were centrifuged at $14,000\times g$ for 4 min at $3 \text{ }^\circ\text{C}$, and the supernatants were collected. Absorbance was measured at 595 nm using bovine albumin as standard.

Determination of superoxide concentration

To determine O_2^- , 1 mL of extract was incubated with 30 mM phosphate buffer [pH 7.6] and 0.51 mM hydroxylamine hydrochloride for 20 min at $25 \text{ }^\circ\text{C}$. Then, 17 mM sulphanilamide and 7 mM α -naphthylamine were added to the incubation mixture for 20 min at $25 \text{ }^\circ\text{C}$. After the reaction, ethyl ether was added in an identical volume and centrifuged at $3000\times g$ for 5 min. The absorbance was measured at 530 nm (Elstner and Heupel 1976).

Extraction of nonenzymatic compounds

Non-enzymatic compounds (H_2O_2 and MDA) were extracted as described by Wu et al. (2006). Briefly, a mixture for extraction of H_2O_2 and MDA was prepared by homogenizing 500 mg of fresh leaf material in 5 mL of 5% (w/v) trichloroacetic acid. Then, the samples were centrifuged at $15,000\times g$ for 15 min at $3 \text{ }^\circ\text{C}$ to collect supernatants.

Determination of hydrogen peroxide concentration

To measure H_2O_2 , 200 μL of supernatant and 1800 μL of reaction mixture (2.5 mM potassium phosphate buffer [pH 7.0] and 500 mM potassium iodide) were mixed, and the absorbance was measured at 390 nm (Velikova et al. 2000).

Quantification of malondialdehyde concentration

MDA was determined by mixing 500 μL of supernatant with 1000 μL of the reaction mixture, which contained 0.5% (w/v) thiobarbituric acid in 20% trichloroacetic acid. The mixture was incubated in boiling water at $95 \text{ }^\circ\text{C}$ for 20 min, with the reaction terminated by placing the reaction container in

an ice bath. The samples were centrifuged at $10,000\times g$ for 10 min, and absorbance was measured at 532 nm. The non-specific absorption at 600 nm subtracted from the absorbance data. The MDA–TBA complex (red pigment) amount was calculated based on the method of Cakmak and Horst (1991), with minor modifications and using an extinction coefficient of $155 \text{ mM}^{-1} \text{ cm}^{-1}$.

Determination of electrolyte leakage

Electrolyte leakage was measured according to the method of Gong et al. (1998) with minor modifications. Fresh tissue (200 mg) was cut into pieces 1 cm in length and placed in containers with 8 mL of distilled deionised water. The containers were incubated in a water bath at $40 \text{ }^\circ\text{C}$ for 30 min, and initial electrical conductivity of the medium (EC_1) was measured. Then, the samples were boiled at $95 \text{ }^\circ\text{C}$ for 20 min to release the electrolytes. After cooling, the final electrical conductivity (EC_2) was measured (Gong et al. 1998). The percentage of electrolyte leakage was calculated using the formula $\text{EL} (\%) = (\text{EC}_1/\text{EC}_2) \times 100$.

Determination of photosynthetic pigments

The chlorophyll and carotenoid determinations were performed with 40 mg of leaf tissue. The samples were homogenized in the dark with 8 mL of 90% methanol (Nuclear). The homogenate was centrifuged at $6000\times g$ for 10 min at $5 \text{ }^\circ\text{C}$. The supernatant was removed, and chlorophyll *a* (Chl *a*) and *b* (Chl *b*), carotenoid (Car) and total chlorophyll (Total Chl) contents were quantified using a spectrophotometer (model UV-M51; Bel Photonics, Italy), according to the methodology of Lichtenthaler and Buschmann (2001).

Measurements of morphological parameters

The growths of roots, stems and leaves were measured based on constant dry mass (g) after drying in a forced-air ventilation oven at $65 \text{ }^\circ\text{C}$.

Determining of Fe and nutrients

Milled samples of 100 mg were weighed in 50-mL conical tubes (Falcon^R, Corning, Mexico) and pre-digested (48 h) with 2 mL of sub-boiled HNO_3 (DST 1000, Savillex, USA). Afterward, 8 mL of a solution containing 4 mL of H_2O_2 (30% v/v, Synth, Brazil) and 4 mL of ultra-pure water (Milli-Q System, Millipore, USA) were added, and the mixture was transferred to a Teflon digestion vessel, closed and heated in a block digester (EasyDigest®, Analab, France) according to the following program: (1) $100 \text{ }^\circ\text{C}$ for 30 min; (2) $150 \text{ }^\circ\text{C}$ for 30 min; (3) $130 \text{ }^\circ\text{C}$ for 10 min; (4) $100 \text{ }^\circ\text{C}$ for 30 min and; and (5) left to cool. The volume was made to 50 mL

with ultra-pure water, and iridium was used as an internal standard at $10 \mu\text{g L}^{-1}$. The determination of nutrients K, Ca, Mg, P, Fe, Mn, Cu, Mo and Zn was carried out using an inductively coupled plasma mass spectrometer (ICP-MS 7900, Agilent, USA). Certified reference materials (NIST 1570a and NIST 1577c) were run in each batch for quality control purposes. All found values were in agreement with certified values.

Data analysis

The data were subjected to an analysis of variance, and significant differences between the means were determined using the Scott–Knott test at a probability level of 5% (Steel et al. 2006). Standard deviations were calculated for each treatment. The statistical analyses were performed with Assistat software.

Results

Fe deficiency was attenuated by the EBR

The application of EBR in *E. urophylla* plants exposed to Fe deficiency significantly increased the Fe content in tissues (Table 1). In the treatment with 100 nM of EBR, increases were on the order of 12% (root), 27% (stem) and 21% (leaf), when compared to the Fe deficiency + 0 EBR treatment (Table 1).

EBR contribution on nutrients contents

Fe deficiency caused significant reductions in the contents of macronutrients (K, Ca, Mg and P) and micronutrients (Mn, Cu, Mo and Zn) in tissues (Table 2). However, the Fe deficiency + 100 nM EBR treatment increased the values of K, Ca, Mg and P in the root (8, 21, 9 and 103%, respectively), in the stem (5, 16, 36 and 12%, respectively), and in the leaf (12, 17, 46 and 23%, respectively) when compared to values obtained in *E. urophylla* plants submitted to Fe

deficiency + 0 nM EBR. The Fe deficiency + 100 nM EBR treatment also promoted increases in the contents of Mn, Cu, Mo and Zn in the root (21, 26, 27 and 25%, respectively), in the stem (28, 11, 100 and 7%, respectively), and in the leaf (16, 28, 25 and 30%, respectively) compared with the Fe deficiency + 0 nM EBR treatment.

EBR mitigated disorders provoked by Fe deficiency on chlorophyll fluorescence

Fe deficiency had negative effects on F_0 , F_m , F_v and F_v/F_m values. With the application of 100 nM EBR, there was a reduction in F_0 (14%) (Fig. 1) and significant increases in F_m (48%), F_v (78%) and F_v/F_m (20%) when compared to plants exposed to Fe deficiency without EBR. Plants under Fe deficiency had significant decreases in Φ_{PSII} , q_p and ETR, while the concentration of 100 nM EBR induced expressive increases of 39, 91 and 38%, respectively, in relation to the Fe deficiency + 0 nM EBR treatment (Table 3). The NPQ, EXC and ETR/ P_N of plants exposed to Fe deficiency showed increases, but when receiving the spray with 100 nM of EBR, there were significant reductions of 19, 14 and 16%, respectively.

Repercussion of Fe deficiency and EBR on gas exchange

Fe deficiency promoted negative repercussions on gas exchange. However, the combined effects of the Fe deficiency + 100 nM EBR treatment induced significant increases in P_N , E , g_s , WUE and P_N/C_i of 63, 11, 50, 48 and 74% respectively, and a decrease of 5% for C_i in the Fe deficiency + 0 nM EBR treatment (Table 4).

Benefits on photosynthetic pigments promoted by the EBR action

Under Fe deficiency, the concentration of 100 nM EBR promoted the maximization of photosynthetic pigments, increasing the levels of Chl *a* (17%), Chl *b* (20%), Total Chl

Table 1 Fe contents in *Eucalyptus urophylla* plants sprayed with EBR and exposed to Fe deficiency

Treatment	EBR (nM)	Fe in root ($\mu\text{g g DM}^{-1}$)	Fe in stem ($\mu\text{g g DM}^{-1}$)	Fe in leaf ($\mu\text{g g DM}^{-1}$)
Control	0	3743 ± 99Aa	34.7 ± 0.8Ba	54.0 ± 1.8Aa
Control	50	3786 ± 84Aa	35.5 ± 0.7Ba	55.1 ± 1.5Aa
Control	100	3807 ± 98Aa	37.5 ± 0.6Aa	55.2 ± 1.2Aa
Fe deficiency	0	1830 ± 44Bb	19.0 ± 0.6Cb	34.9 ± 1.1Cb
Fe deficiency	50	2041 ± 86Ab	21.2 ± 0.5Bb	38.0 ± 0.7Bb
Fe deficiency	100	2051 ± 57Ab	24.2 ± 0.8Ab	42.3 ± 1.7Ab

Fe Iron. Columns with different uppercase letters between EBR levels (0, 50 and 100 nM EBR under equal Fe concentration) and lowercase letters between Fe levels (control and Fe deficiency under equal EBR concentration) indicate significant differences from the Scott–Knott test ($p < 0.05$). Means ± SD, $n = 5$

Table 2 Nutrient contents in *Eucalyptus urophylla* plants sprayed with EBR and exposed to Fe deficiency

Treatment	EBR (nM)	K (mg g DM ⁻¹)	Ca (mg g DM ⁻¹)	Mg (mg g DM ⁻¹)	P (mg g DM ⁻¹)	Mn (μg g DM ⁻¹)	Cu (μg g DM ⁻¹)	Mo (μg g DM ⁻¹)	Zn (μg g DM ⁻¹)
Contents in root									
Control	0	23.8±0.1Aa	20.3±0.7Aa	5.4±0.4Aa	19.0±1.4Aa	51.3±3.1Aa	18.6±0.3Ba	70.4±2.5Aa	44.8±0.8Ba
Control	50	24.0±1.4Aa	20.6±0.9Aa	5.5±0.3Aa	19.1±0.8Aa	52.6±1.0Aa	19.2±0.4Ba	71.7±2.8Aa	45.5±0.7Ba
Control	100	24.2±1.7Aa	20.8±0.9Aa	5.5±0.4Aa	19.5±0.9Aa	53.7±2.3Aa	20.5±0.5Aa	72.6±2.1Aa	47.6±0.9Aa
Fe deficiency	0	20.9±1.7Ab	11.8±0.4Bb	3.3±0.2Ab	9.2±0.5Cb	38.5±0.5Bb	13.6±0.5Cb	50.6±1.4Cb	30.7±0.7Cb
Fe deficiency	50	22.4±1.0Aa	13.6±0.8Ab	3.5±0.2Ab	11.7±0.7Bb	46.1±1.2Ab	15.2±0.7Bb	57.9±1.1Bb	36.8±0.7Bb
Fe deficiency	100	22.5±1.0Aa	14.3±0.6Ab	3.6±0.2Ab	18.7±0.8Aa	46.6±1.3Ab	17.2±0.5Ab	64.4±1.5Ab	38.4±0.5Ab
Contents in stem									
Control	0	17.1±0.8Aa	8.8±0.4Aa	1.6±0.1Aa	4.8±0.3Aa	68.1±1.0Aa	5.8±0.1Ba	2.0±0.1Ba	11.8±0.3Aa
Control	50	17.2±0.6Aa	8.8±0.3Aa	1.6±0.1Aa	5.0±0.1Aa	68.8±1.8Aa	6.1±0.1Aa	2.4±0.1Aa	11.9±0.5Aa
Control	100	17.3±0.5Aa	9.0±0.3Aa	1.8±0.1Aa	5.0±0.1Aa	69.9±3.6Aa	6.2±0.1Aa	2.4±0.1Aa	12.3±0.3Aa
Fe deficiency	0	14.9±0.8Ab	6.7±0.3Bb	1.1±0.1Bb	4.2±0.2Bb	44.3±0.6Bb	4.7±0.1Bb	0.6±0.1Cb	8.6±0.3Bb
Fe deficiency	50	15.5±0.7Ab	7.6±0.3Ab	1.2±0.1Bb	4.4±0.1Bb	54.5±0.9Ab	4.8±0.1Bb	0.9±0.1Bb	9.1±0.1Ab
Fe deficiency	100	15.7±0.6Ab	7.8±0.2Ab	1.5±0.1Ab	4.7±0.1Ab	56.5±1.2Ab	5.2±0.2Ab	1.2±0.1Ab	9.2±0.1Ab
Contents in leaf									
Control	0	15.3±0.4Aa	7.3±0.5Aa	1.9±0.1Ba	3.2±0.2Aa	283.7±7.2Ba	5.9±0.1Aa	5.3±0.1Ca	17.9±0.6Aa
Control	50	15.7±0.5Aa	7.5±0.4Aa	1.9±0.1Ba	3.3±0.1Aa	293.4±6.8Ba	6.0±0.3Aa	5.6±0.1Ba	17.9±0.6Aa
Control	100	15.9±0.5Aa	7.6±0.1Aa	2.2±0.1Aa	3.4±0.2Aa	307.2±5.7Aa	6.1±0.3Aa	5.9±0.1Aa	18.3±0.5Aa
Fe deficiency	0	12.9±0.4Bb	5.2±0.2Bb	1.3±0.1Cb	2.6±0.1Bb	236.3±6.1Bb	3.6±0.1Bb	3.2±0.1Cb	9.3±0.3Cb
Fe deficiency	50	14.3±0.5Ab	5.7±0.1Ab	1.6±0.1Bb	3.0±0.1Ab	270.2±10.0Ab	4.3±0.1Ab	3.6±0.1Bb	10.7±0.3Bb
Fe deficiency	100	14.4±0.6Ab	6.1±0.4Ab	1.9±0.1Ab	3.2±0.1Aa	273.3±7.2Ab	4.6±0.2Ab	4.0±0.1Ab	12.1±0.2Ab

Columns with different uppercase letters between EBR levels (0, 50 and 100 nM EBR under equal Fe concentration) and lowercase letters between Fe levels (control and Fe deficiency under equal EBR concentration) indicate significant differences from the Scott–Knott test ($p < 0.05$). Means ± SD, $n = 5$

K Potassium, Ca calcium, Mg magnesium, P phosphorus, Mn manganese, Cu copper, Mo molybdenum, Zn zinc

(17%) and Car (45%) compared to treatment with Fe deficiency without EBR (0 nM). In addition, there were reductions in the Chl *a*/Chl *b* ratio and Total Chl/Car ratio of 2 and 15%, respectively (Table 5).

Effects of EBR on oxidant compounds and cell damages

The oxidant compounds (O_2^- and H_2O_2) and indicators of cell damages (MDA and EL) in plants with Fe deficiency suffered increases in their concentrations. However, the application of 100 nM EBR occurred with reductions in levels of O_2^- (35%), H_2O_2 (28%), MDA (28%) and EL (17%), when compared to the Fe deficiency + 0 nM of EBR treatment (Fig. 2).

Growth of *E. urophylla* plants treated with EBR

Plants under Fe deficiency presented slight improvement ($p \geq 0.05$) on morphological variables when receiving EBR application, showing increases for LDM, RDM, SDM and TDM (1, 5, 2 and 2%, respectively) at a concentration of 100 nM of EBR, compared to the Fe deficiency + 0 nM of EBR treatment (Fig. 3).

Discussion

The Fe content reduction described in *E. urophylla* plants corroborates the deficiency of this nutrient, but the application of 100 nM EBR induced a significant increase in

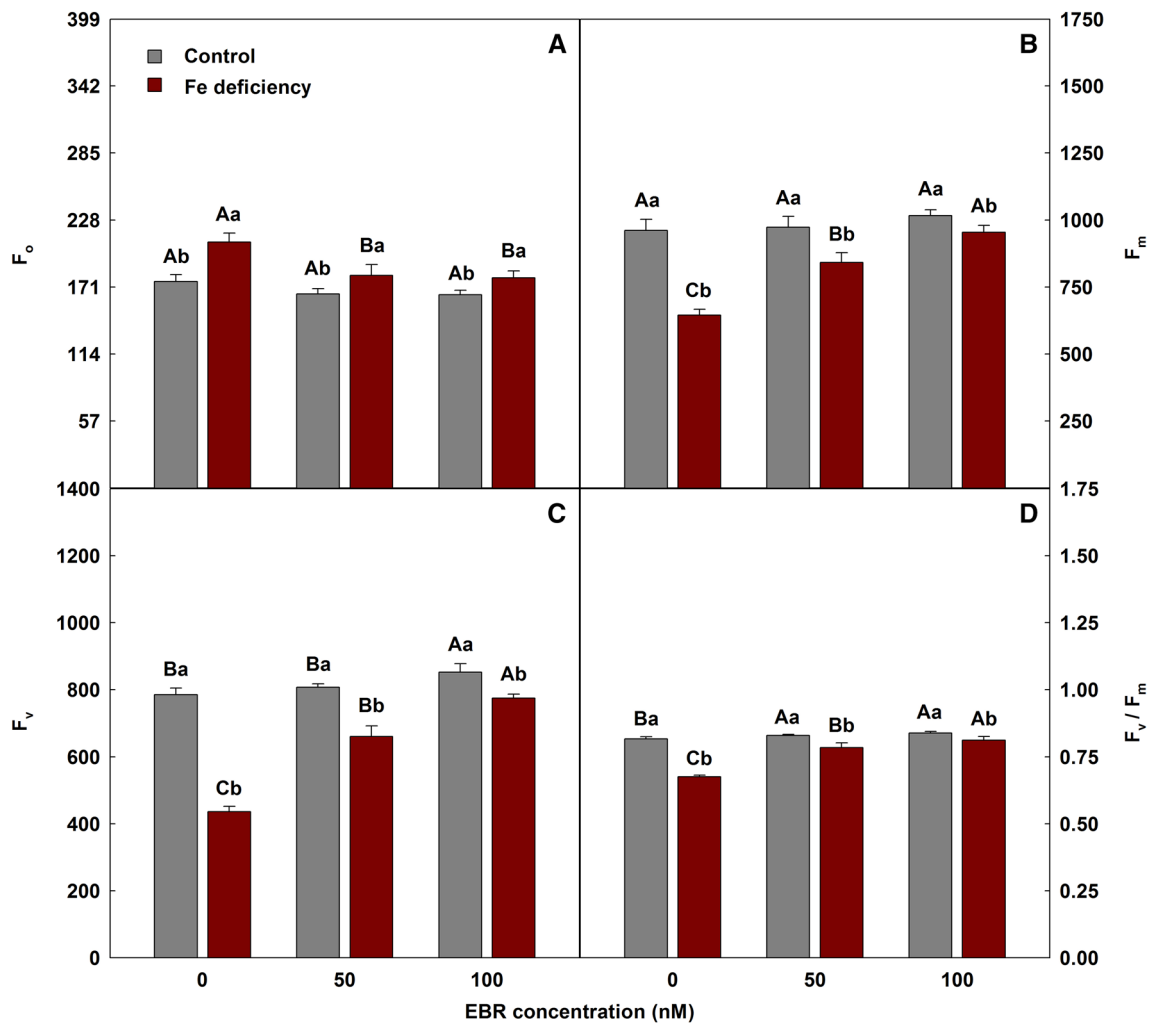


Fig. 1 Minimal fluorescence yield of the dark-adapted state (F_0), maximal fluorescence yield of the dark-adapted state (F_m), variable fluorescence (F_v) and maximal quantum yield of PSII photochemistry (F_v/F_m) in *Eucalyptus urophylla* plants sprayed with EBR and exposed to Fe deficiency. Different uppercase letters between EBR

levels (0, 50 and 100 nM EBR under equal Fe concentration) and lowercase letters between Fe levels (control and Fe deficiency under equal EBR concentration) indicate significant differences from the Scott–Knott test ($p < 0.05$). Means \pm SD, $n = 5$

Table 3 Chlorophyll fluorescence in *Eucalyptus urophylla* plants sprayed with EBR and exposed to Fe deficiency

Treatment	EBR (nM)	Φ_{PSII}	q_P	NPQ	ETR ($\mu\text{mol m}^{-2} \text{s}^{-1}$)	EXC ($\mu\text{mol m}^{-2} \text{s}^{-1}$)	ETR/ P_N
Control	0	0.49 ± 0.01 Ba	0.79 ± 0.04 Ba	0.35 ± 0.02 Ab	72.7 ± 2.0 Ba	0.39 ± 0.02 Ab	7.6 ± 0.2 Ab
Control	50	0.50 ± 0.01 Ba	0.83 ± 0.03 Ba	0.35 ± 0.01 Ab	73.7 ± 1.1 Ba	0.38 ± 0.02 Ab	6.9 ± 0.5 Bb
Control	100	0.54 ± 0.01 Aa	0.88 ± 0.01 Aa	0.34 ± 0.01 Ab	79.8 ± 2.1 Aa	0.35 ± 0.02 Ab	6.8 ± 0.3 Ba
Fe deficiency	0	0.33 ± 0.02 Bb	0.33 ± 0.02 Bb	0.72 ± 0.04 Aa	48.9 ± 2.7 Bb	0.51 ± 0.03 Aa	8.5 ± 0.4 Aa
Fe deficiency	50	0.43 ± 0.03 Ab	0.58 ± 0.04 Ab	0.61 ± 0.03 Ba	63.5 ± 2.5 Ab	0.45 ± 0.02 Ba	7.8 ± 0.2 Ba
Fe deficiency	100	0.46 ± 0.02 Ab	0.63 ± 0.04 Ab	0.58 ± 0.02 Ba	67.4 ± 2.2 Ab	0.44 ± 0.02 Ba	7.1 ± 0.3 Ca

Columns with different uppercase letters between EBR levels (0, 50 and 100 nM EBR under equal Fe concentration) and lowercase letters between Fe levels (control and Fe deficiency under equal EBR concentration) indicate significant differences from the Scott–Knott test ($p < 0.05$). Means \pm SD, $n = 5$

Φ_{PSII} Effective quantum yield of PSII photochemistry, q_P photochemical quenching coefficient, NPQ nonphotochemical quenching, ETR electron transport rate, EXC relative energy excess at the PSII level, ETR/ P_N ratio between the electron transport rate and net photosynthetic rate

Table 4 Gas exchange in *Eucalyptus urophylla* plants sprayed with EBR and exposed to Fe deficiency

Treatment	EBR (nM)	P_N ($\mu\text{mol m}^{-2} \text{s}^{-1}$)	E ($\text{mmol m}^{-2} \text{s}^{-1}$)	g_s ($\text{mol m}^{-2} \text{s}^{-1}$)	C_i ($\mu\text{mol mol}^{-1}$)	WUE ($\mu\text{mol mmol}^{-1}$)	P_N/C_i ($\mu\text{mol m}^{-2} \text{s}^{-1} \text{Pa}^{-1}$)
Control	0	9.5 ± 0.2Ca	1.85 ± 0.06Ba	0.11 ± 0.01Ba	221 ± 7Ab	5.1 ± 0.1Ba	0.043 ± 0.001Ca
Control	50	10.7 ± 0.3Ba	2.04 ± 0.08Aa	0.14 ± 0.01Aa	214 ± 9Ab	5.2 ± 0.2Ba	0.050 ± 0.002Ba
Control	100	11.7 ± 0.5Aa	2.06 ± 0.08Aa	0.15 ± 0.01Aa	214 ± 5Ab	5.7 ± 0.2Aa	0.055 ± 0.002Aa
Fe deficiency	0	5.7 ± 0.4Cb	1.71 ± 0.05Bb	0.08 ± 0.01Bb	248 ± 5Aa	3.3 ± 0.2Cb	0.023 ± 0.001Cb
Fe deficiency	50	8.1 ± 0.7Bb	1.86 ± 0.04Ab	0.11 ± 0.01Ab	235 ± 6Ba	4.3 ± 0.3Bb	0.034 ± 0.002Bb
Fe deficiency	100	9.3 ± 0.3Ab	1.90 ± 0.06Ab	0.12 ± 0.01Ab	235 ± 4Ba	4.9 ± 0.1Ab	0.040 ± 0.002Ab

P_N Net photosynthetic rate, E transpiration rate, g_s stomatal conductance, C_i intercellular CO_2 concentration, WUE water-use efficiency, P_N/C_i carboxylation instantaneous efficiency

Columns with different uppercase letters between EBR levels (0, 50 and 100 nM EBR under equal Fe concentration) and lowercase letters between Fe levels (control and Fe deficiency under equal EBR concentration) indicate significant differences from the Scott–Knott test ($p < 0.05$)

Means ± SD, $n = 5$

Table 5 Photosynthetic pigments in *Eucalyptus urophylla* plants sprayed with EBR and exposed to Fe deficiency

Treatment	EBR (nM)	Chl <i>a</i> (mg g^{-1} FM)	Chl <i>b</i> (mg g^{-1} FM)	Total Chl (mg g^{-1} FM)	Car (mg g^{-1} FM)	Ratio Chl <i>a</i> /Chl <i>b</i>	Ratio Total Chl/Car
Control	0	10.9 ± 0.4Aa	2.3 ± 0.1Ba	13.3 ± 0.5Aa	0.35 ± 0.02Ba	4.4 ± 0.3Aa	37.9 ± 1.3Aa
Control	50	11.3 ± 0.6Aa	2.6 ± 0.1Aa	13.9 ± 0.5Aa	0.39 ± 0.01Aa	4.3 ± 0.2Aa	36.9 ± 1.8Aa
Control	100	11.6 ± 0.8Aa	2.7 ± 0.1Aa	14.3 ± 0.7Aa	0.40 ± 0.01Aa	4.3 ± 0.3Aa	36.9 ± 1.4Aa
Fe deficiency	0	7.1 ± 0.2Bb	1.5 ± 0.1Ba	8.6 ± 0.3Bb	0.22 ± 0.01Cb	4.6 ± 0.2Aa	38.5 ± 1.1Aa
Fe deficiency	50	8.1 ± 0.4Ab	1.8 ± 0.1Ab	9.9 ± 0.5Ab	0.28 ± 0.01Bb	4.5 ± 0.2Aa	35.6 ± 1.3Ba
Fe deficiency	100	8.3 ± 0.5Ab	1.8 ± 0.1Ab	10.1 ± 0.6Ab	0.32 ± 0.02Ab	4.5 ± 0.2Aa	32.6 ± 1.1Cb

Chl *a* Chlorophyll *a*, Chl *b* chlorophyll *b*, Total chl total chlorophyll, Car carotenoids

Columns with different uppercase letters between EBR levels (0, 50 and 100 nM EBR under equal Fe concentration) and lowercase letters between Fe levels (control and Fe deficiency under equal EBR concentration) indicate significant differences from the Scott–Knott test ($p < 0.05$)

Means ± SD, $n = 5$

Fe concentration, indicating that this steroid improved the absorption, transport and accumulation of Fe in the evaluated tissues. EBR induces Fe uptake, increasing the activity of the H^+ -ATPase enzyme in roots (Song et al. 2016), which under normal conditions are responsible for increasing Fe content and transport of protons out of the cell through the membrane (Santi et al. 2005; Gévaudant et al. 2007). Additionally, Wang et al. (2015) confirmed that in *Arachis hypogaea* L. plants, EBR plays the role of a signalization molecule in response to Fe deficiency, regulating long-distance transport and Fe translocation from roots to shoots. Kong et al. (2015) verified that Fe deficiency reduced Fe content in root and stem by 39 and 17%, respectively.

Plants sprayed with EBR under Fe deficiency had increases in macronutrient (K, Ca, Mg and P) and micronutrient contents (Mn, Cu, Mo and Zn). These results confirm that EBR mitigates the effects of Fe deficiency, optimizing the processes of ion absorption and assimilation, which implies a maintenance of nutritional balance (Talaat and Shawky 2013). Additionally, Wang et al. (2012) verified that Fe deficiency induces a decrease in pH of the

growth medium, provoking low solubility of nutrients and negatively interfering with absorption of other elements. Talaat and Abdallah (2010) showed that EBR promoted significant increases in N (19%), P (11%), K (24%), Zn (13%), Mn (10%) and Cu (7%) when evaluating the Sakha 1 cultivar of *Vicia faba* L.

The application of EBR (100 nM) mitigated the negative effects of Fe deficiency under F_0 , F_m , F_v and F_v/F_m in *E. urophylla* plants. These results demonstrate that EBR promotes a reduction of the intensity of photoinhibition in the plants, avoiding damages to reaction centre II and increasing the excitation energy transfer capacity of the antenna to PSII, resulting in the improvement of photosynthetic machinery performance (Baker and Rosenqvist 2004; Hayat et al. 2010). F_v/F_m is frequently used to indicate photoinhibition or stress conditions in PSII (Calatayud and Barreno 2004). The physiological variables F_0 , F_m and F_v/F_m in *Capsicum annum* L. plants showed increases after application of EBR (0.5 mg L^{-1}) in the research conducted by Houimli et al. (2008).

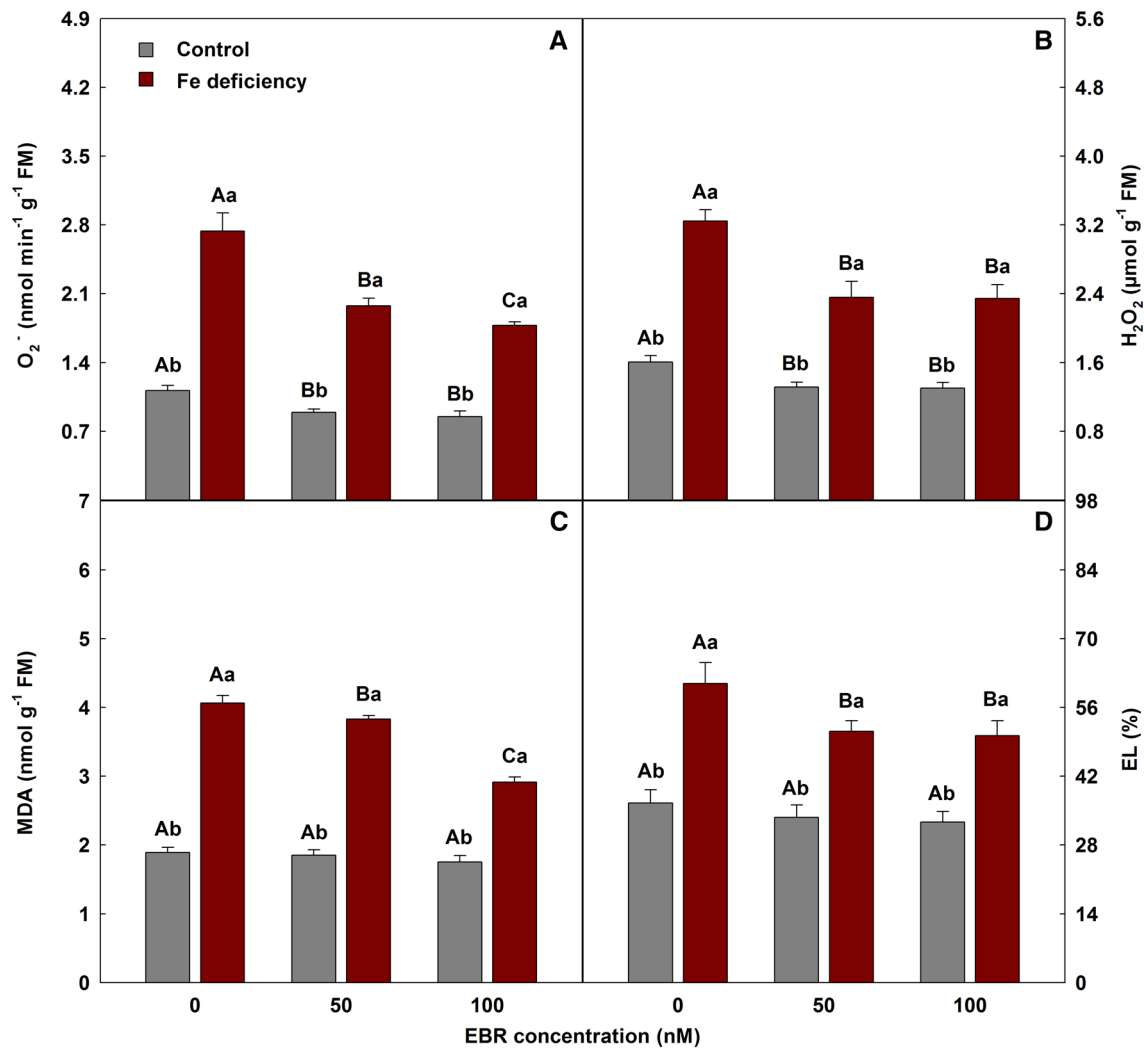


Fig. 2 Superoxide (O_2^-), hydrogen peroxide (H_2O_2), malondialdehyde (MDA) and electrolyte leakage (EL) in *Eucalyptus urophylla* plants sprayed with EBR and exposed to Fe deficiency. Different uppercase letters between EBR levels (0, 50 and 100 nM EBR under

equal Fe concentration) and lowercase letters between Fe levels (control and Fe deficiency under equal EBR concentration) indicate significant differences from the Scott–Knott test ($p < 0.05$). Means \pm SD, $n = 5$

EBR increased the values of Φ_{PSII} , q_P and ETR in plants under Fe deficiency due to positive effects of F_0 and F_m . This result indicates a greater dissipation of fluorescence by processes related to electron transport in the chloroplasts and consequent generation of ATP and NADPH, reflected in a higher P_N (Kumari et al. 2017). ETR was positively influenced by EBR because this steroid increased the activity of the *Cyt-b_{6/f}* complex and Fd. *Cyt-b_{6/f}* and Fd are plant proteins with vital functions in photosynthesis, both using Fe as a structural element (Buonasera et al. 2011). *Cyt-b_{6/f}* is responsible for the transference of electrons from PSII to PSI, generating an electrochemical gradient of protons in the membrane used during ATP synthesis (Kurisu et al. 2002). In addition, Fd is a protein composed of Fe and S (Fe–S protein) (Balk and Lobréaux 2005) and is responsible

for donating electrons to the processes of photosynthesis and reduction of $NADP^+$ to NADPH (Fromme et al. 2003; Ceccarelli et al. 2004; Merchant and Helmann 2012). Yuan et al. (2012) detected increases in Φ_{PSII} and q_P , promoted by EBR (0.1 μ M), in *Cucumis sativus* L. plants, while Xia et al. (2009) verified increases to Φ_{PSII} and q_P of 16 and 18%, respectively, in *Cucumis sativus* plants treated with 0.1 μ M EBR.

EBR promoted reductions in NPQ, EXC and ETR/P_N in plants exposed to Fe deficiency. Reductions indicate that EBR stimulated a plant protection mechanism against over-excitation, decreasing the intensity of excitation energy dissipation in the PSII antenna in the form of heat, and consequently avoiding photoinhibition in the leaves of *E. urophylla* (Stepien and Johnson 2009). A decrease in EXC is

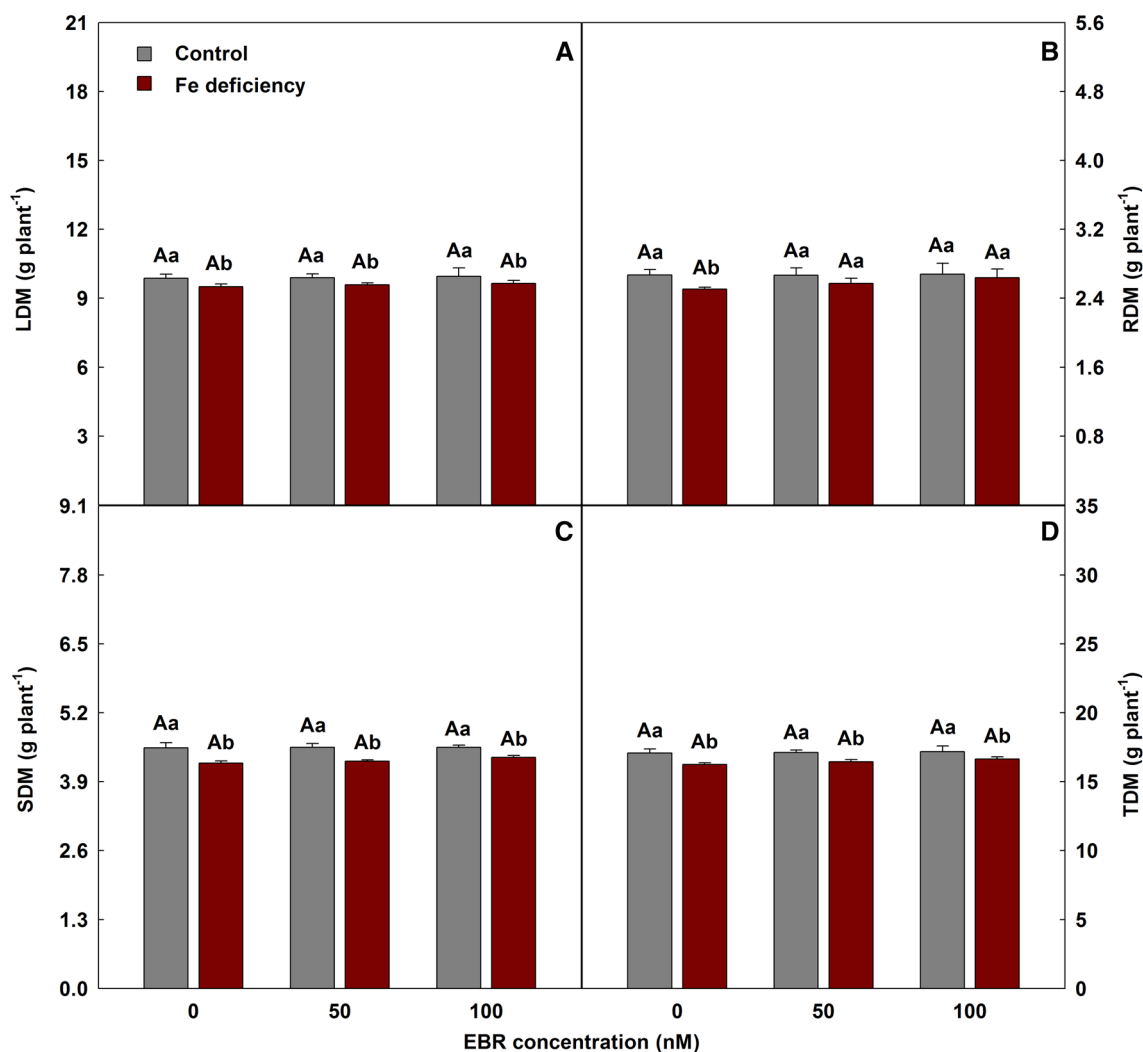


Fig. 3 Leaf dry matter (LDM), root dry matter (RDM), stem dry matter (SDM) and total dry matter (TDM) in *Eucalyptus urophylla* plants sprayed with EBR and exposed to Fe deficiency. Different uppercase letters between EBR levels (0, 50 and 100 nM EBR under equal Fe

concentration) and lowercase letters between Fe levels (control and Fe deficiency under equal EBR concentration) indicate significant differences from the Scott–Knott test ($p < 0.05$). Means \pm SD, $n = 5$

a result of the decrease in NPQ, showing that EBR reduced the photochemical damages on PSII (Silva et al. 2012). Decreases in ETR/P_N suggest that EBR minimized the alternative drains of electrons, and as a consequence, minimized the Mehler reactions and photorespiration process, which induced a better use of electrons in the photochemical activity (Jesus et al. 2017).

In this study, EBR mitigated Fe deficiency in *E. urophylla*, minimizing negative effects under gas exchange. EBR positively modulated P_N , E and C_i due to better performance in g_s (Yu et al. 2004). In addition, EBR also improved the carboxylation rate of RuBisCO (Hasan et al. 2011), and consequently promoted a better efficiency of CO_2 fixation in the Calvin–Benson cycle in chloroplasts, decreasing the intercellular CO_2 concentration (C_i) (Yu et al. 2004). The

increases obtained for WUE are explained by the improvements promoted by EBR under P_N and E , with WUE calculated by the relation between variables P_N and E (Barros Junior et al. 2017). Increases of 28, 28, 18 and 63% for P_N , E and C_i and g_s , respectively, were verified by Yusuf et al. (2014) on cultivar T-44 of *Vigna radiata* (L.) R. Wilczek after receiving an application of 10^{-6} M of 28-homobrassinolide. Farooq et al. (2009) reported an increase of 3% in WUE and a decrease of 19% to P_N/C_i in *Oryza sativa* L. plants treated with EBR (0.01 μ M) via leaf.

EBR caused reductions in O_2^- , H_2O_2 , MDA and EL levels of plants exposed to Fe deficiency. These reductions confirm that EBR acts as a secondary messenger, signaling to increase the activity of antioxidant enzymes (SOD, CAT, APX and POX). These enzymes are responsible for

cellular detoxification, controlling the production of reactive oxygen species (ROS) such as O_2^- and H_2O_2 (Arora et al. 2008; El-Beltagi and Mohamed 2013) that may be caused by Fe deficiency (Verma and Pandey 2016). Low ROS production also implies on reduction of MDA and EL because EBR also positively influences membrane properties linked to permeability, integrity and stability (Sharma and Bhardwaj 2007; Shahbaz et al. 2008). Song et al. (2016) found a decrease in O_2^- , H_2O_2 and MDA contents in the leaf promoted by EBR (5×10^{-7} M) on the order of 20, 18 and 27%, respectively, in *Arachis hypogaea* L. plants under Fe deficiency (10^{-5} M EDTA-Fe).

The foliar application of 100 nM EBR in *E. urophylla* plants exposed to Fe deficiency resulted in increases in Chl *a*, Chl *b*, Total Chl and Car levels, evidence that EBR mitigated the oxidative damages caused to chloroplast membranes (MDA and EL) and decreased the accumulations of O_2^- and H_2O_2 (Lima and Lobato 2017). Higher rates of photosynthetic pigments are also a result of the maintenance of Fe content in tissues promoted by EBR because Fe plays an important role in the formation of δ -aminolevulinic acid, a precursor of chlorophyll biosynthesis, an essential component for maintenance of the structure and function of chloroplasts (Rout and Sahoo 2015). Li et al. (2012) showed increases in Chl *a* and Total Chl levels in *Chorispora bungeana* Fisch. & C.A. Mey plants after exogenous application of EBR. With respect to Chl *b* and Car, Honnerová et al. (2010) found increases of 13 and 3%, respectively, in *Zea mays* L. plants treated with 10^{-14} M of EBR.

After EBR application, Chl *a*/Chl *b* and Chl *a*/Car ratios presented lower values due to higher Chl *b* and Car as compared to Chl *a*. Houimli et al. (2010) showed that EBR (0.5 mg L^{-1}) application promoted a reduction in the Chl *a*/Chl *b* ratio of *Capsicum annum* plants.

After EBR application, plants exposed to Fe deficiency had increases linked to growth (LDM, RDM, SDM and TDM). These increases are explained by the EBR stimulating the processes of cell division and elongation, combined with adequate nutrient contents and higher photosynthetic rates (Shahbaz and Ashraf 2007), which results in the accumulation of dry matter (Bhardwaj et al. 2007). Swamy and Rao (2006) studied *Pelargonium graveolens* L'Hér. plants treated with 100 μM EBR and detected increases of 84 and 40% in LDM and RDM, respectively. Sharma et al. (2008) evaluated *Triticum aestivum* L. at harvest stage and obtained an increase to TDM of 11% after application of EBR (0.5 ppm). For shoot tissue (leaf + stem), Ogwenó et al. (2008) reported an increase of approximately 16% for *Lycopersicon esculentum* L. exposed to the application of 0.1 mg L^{-1} EBR.

Conclusions

Our results clearly revealed that EBR attenuated the negative effects caused by Fe deficiency on nutritional status and in the physiological and biochemical behaviours of *E. urophylla* plants, increasing the contents of macronutrients and micronutrients, including Fe. EBR also improved the photochemical efficiency of PSII, gas exchange and photosynthetic pigments, inducing minor accumulations of oxidative compounds. Additionally, *E. urophylla* plants submitted to 100 nM of EBR had better nutritional, biochemical, physiological and morphological results.

Author contribution statement AKSL was advisor of this project, planning all phases of this research. MDRL and UOBJ conducted the experiment in the greenhouse and performed physiological, biochemical and morphological determinations. BLB carried out nutritional determinations and helped in drafting the manuscript and in interpreting the results.

Acknowledgements This research had financial support from Fundação Amazônia de Amparo a Estudos e Pesquisas (FAPESPA/Brazil), Conselho Nacional de Desenvolvimento Científico e Tecnológico (CNPq/Brazil) and Universidade Federal Rural da Amazônia (UFRA/Brazil) to AKSL. MDRL and UOBJ were supported by scholarships from Universidade Federal Rural da Amazônia (UFRA/Brazil).

Compliance with ethical standards

Conflict of interest The authors declare that they have no conflict of interest.

References

- Abadía J, Morales F, Abadía A (1999) Photosystem II efficiency in low chlorophyll, iron-deficient leaves. *Plant Soil* 215:183–192. <https://doi.org/10.1023/A:1004451728237>
- Abdullahi BA, Gu X, Gan Q, Yang Y (2003) Brassinolide amelioration of aluminum toxicity in mungbean seedling growth. *J Plant Nutr* 26:1725–1734. <https://doi.org/10.1081/PLN-120023278>
- Ahmed GJ, Choudhary SP, Chen S et al (2013) Role of brassinosteroids in alleviation of phenanthrene–cadmium co-contamination-induced photosynthetic inhibition and oxidative stress in tomato. *J Exp Bot* 64:199–213. <https://doi.org/10.1093/jxb/ers323>
- Arora N, Bhardwaj R, Sharma P, Arora HK (2008) Effects of 28-homobrassinolide on growth, lipid peroxidation and antioxidant enzyme activities in seedlings of *Zea mays* L. under salinity stress. *Acta Physiol Plant* 30:833–839. <https://doi.org/10.1007/s11738-008-0188-9>
- Badawi GH, Yamauchi Y, Shimada E et al (2004) Enhanced tolerance to salt stress and water deficit by overexpressing superoxide dismutase in tobacco (*Nicotiana tabacum*) chloroplasts. *Plant Sci* 166:919–928. <https://doi.org/10.1016/j.plantsci.2003.12.007>

- Bajguz A (2000) Effect of brassinosteroids on nucleic acids and protein content in cultured cells of *Chlorella vulgaris*. *Plant Physiol Biochem* 38:209–215. [https://doi.org/10.1016/S0981-9428\(00\)00733-6](https://doi.org/10.1016/S0981-9428(00)00733-6)
- Bajguz A, Hayat S (2009) Effects of brassinosteroids on the plant responses to environmental stresses. *Plant Physiol Biochem* 47:1–8. <https://doi.org/10.1016/j.plaphy.2008.10.002>
- Baker NR, Rosenqvist E (2004) Applications of chlorophyll fluorescence can improve crop production strategies: an examination of future possibilities. *J Exp Bot* 55:1607–1621. <https://doi.org/10.1093/jxb/erh196>
- Baker HM, Anderson BF, Baker EN (2003) Dealing with iron: common structural principles in proteins that transport iron and heme. *Proc Natl Acad Sci* 100:3579–3583. <https://doi.org/10.1073/pnas.0637295100>
- Balk J, Lobréaux S (2005) Biogenesis of iron–sulfur proteins in plants. *Trends Plant Sci* 10:324–331. <https://doi.org/10.1016/j.tplants.2005.05.002>
- Barros Junior UO, Barbosa MAM, Lima MDR et al (2017) Short-time of rehydration is not effective to re-establish chlorophyll fluorescence and gas exchange in two cowpea cultivars submitted to water deficit. *Not Bot Horti Agrobot Cluj Napoca* 45:238–244. <https://doi.org/10.15835/nbha45110569>
- Bhardwaj R, Arora N, Sharma P, Arora HK (2007) Effects of 28-homobrassinolide on seedling growth, lipid peroxidation and antioxidative enzyme activities under nickel stress in seedlings of *Zea mays* L. *Asian J Plant Sci* 6:765–772. <https://doi.org/10.3923/ajps.2007.765.772>
- Bishop GJ, Koncz C (2002) Brassinosteroids and plant steroid hormone signaling. *Plant Cell* 14:S97–S110. <https://doi.org/10.1105/tpc.001461>
- Buonassera K, Lambrea M, Rea G et al (2011) Technological applications of chlorophyll a fluorescence for the assessment of environmental pollutants. *Anal Bioanal Chem* 401:1139–1151. <https://doi.org/10.1007/s00216-011-5166-1>
- Cakmak I, Horst WJ (1991) Effect of aluminium on lipid peroxidation, superoxide dismutase, catalase, and peroxidase activities in root tips of soybean (*Glycine max*). *Physiol Plant* 83:463–468. <https://doi.org/10.1111/j.1399-3054.1991.tb00121.x>
- Calatayud A, Barreno E (2004) Response to ozone in two lettuce varieties on chlorophyll a fluorescence, photosynthetic pigments and lipid peroxidation. *Plant Physiol Biochem* 42:549–555. <https://doi.org/10.1016/j.plaphy.2004.05.002>
- Ceccarelli EA, Arakaki AK, Cortez N, Carrillo N (2004) Functional plasticity and catalytic efficiency in plant and bacterial ferredoxin-NADP(H) reductases. *Biochim Biophys Acta* 1698:155–165. <https://doi.org/10.1016/j.bbapap.2003.12.005>
- Clouse SD (2002) Brassinosteroids—plant counterparts to animal steroid hormones? *Vitam Horm* 65:195–223. [https://doi.org/10.1016/S0083-6729\(02\)65065-4](https://doi.org/10.1016/S0083-6729(02)65065-4)
- Clouse SD, Sasse JM (1998) Brassinosteroids: essential regulators of plant growth and development. *Annu Rev Plant Physiol Plant Mol Biol* 49:427–451. <https://doi.org/10.1146/annurev.arplant.49.1.427>
- El-Beltagi HS, Mohamed HI (2013) Reactive oxygen species, lipid peroxidation and antioxidative defense mechanism. *Not Bot Horti Agrobot Cluj Napoca* 41:44–57. <https://doi.org/10.15835/nbha4118929>
- Elstner EF, Heupel A (1976) Inhibition of nitrite formation from hydroxylammonium chloride: a simple assay for superoxide dismutase. *Anal Biochem* 70:616–620. [https://doi.org/10.1016/0003-2697\(76\)90488-7](https://doi.org/10.1016/0003-2697(76)90488-7)
- Eskandari H (2011) The importance of iron (Fe) in plant products and mechanism of its uptake by plants. *J Appl Environ Biol Sci* 1:448–452
- Farooq M, Wahid A, Basra SMA, Islam-ud-Din (2009) Improving water relations and gas exchange with brassinosteroids in rice under drought stress. *J Agron Crop Sci* 195:262–269. <https://doi.org/10.1111/j.1439-037X.2009.00368.x>
- Fromme P, Melkozernov A, Jordan P, Krauss N (2003) Structure and function of photosystem I: interaction with its soluble electron carriers and external antenna systems. *FEBS Lett* 555:40–44. [https://doi.org/10.1016/S0014-5793\(03\)01124-4](https://doi.org/10.1016/S0014-5793(03)01124-4)
- Fujioka S, Yokota T (2003) Biosynthesis and metabolism of brassinosteroids. *Annu Rev Plant Biol* 54:137–164. <https://doi.org/10.1146/annurev.arplant.54.031902.134921>
- Gévaudant F, Duby G, von Stedingk E et al (2007) Expression of a constitutively activated plasma membrane H⁺-ATPase alters plant development and increases salt tolerance. *Plant Physiol* 144:1763–1776. <https://doi.org/10.1104/pp.107.1.03762>
- Giehl RF, Meda AR, Wirén NV (2009) Moving up, down, and everywhere: signaling of micronutrients in plants. *Curr Opin Plant Biol* 12:320–327. <https://doi.org/10.1016/j.pbi.2009.04.006>
- Gonçalves JLM, Stape JL, Laclau JP et al (2008) Assessing the effects of early silvicultural management on long-term site productivity of fast-growing eucalypt plantations: the Brazilian experience. *South For* 70:105–118. <https://doi.org/10.2989/SOUTH.FOR.2008.70.2.6.534>
- Gong M, Li Y-J, Chen S-Z (1998) Abscisic acid-induced thermotolerance in maize seedlings is mediated by calcium and associated with antioxidant systems. *J Plant Physiol* 153:488–496. [https://doi.org/10.1016/S0176-1617\(98\)80179-X](https://doi.org/10.1016/S0176-1617(98)80179-X)
- Grattapaglia D, Kirst M (2008) *Eucalyptus* applied genomics: from gene sequences to breeding tools. *New Phytol* 179:911–929. <https://doi.org/10.1111/j.1469-8137.2008.02503.x>
- Guerinot ML (2001) Improving rice yields: ironing out the details. *Nat Biotechnol* 19:417–418. <https://doi.org/10.1038/88067>
- Guerinot ML, Yi Y (1994) Iron: nutritious, noxious, and not readily available. *Plant Physiol* 104:815–820. <https://doi.org/10.1104/pp.104.3.815>
- Hänsch R, Mendel RR (2009) Physiological functions of mineral micronutrients (Cu, Zn, Mn, Fe, Ni, Mo, B, Cl). *Curr Opin Plant Biol* 12:259–266. <https://doi.org/10.1016/j.pbi.2009.05.006>
- Hasan SA, Hayat S, Ahmad A (2011) Brassinosteroids protect photosynthetic machinery against the cadmium induced oxidative stress in two tomato cultivars. *Chemosphere* 84:1446–1451. <https://doi.org/10.1016/j.chemosphere.2011.04.047>
- Hayat S, Hasan SA, Yusuf M et al (2010) Effect of 28-homobrassinolide on photosynthesis, fluorescence and antioxidant system in the presence or absence of salinity and temperature in *Vigna radiata*. *Environ Exp Bot* 69:105–112. <https://doi.org/10.1016/j.envexpbot.2010.03.004>
- Hoagland DR, Arnon DI (1950) The water-culture method for growing plants without soil, 2nd edn. California Agricultural Experiment Station, Berkeley
- Honnerová J, Rothová O, Holá D et al (2010) The exogenous application of brassinosteroids to *Zea mays* (L.) stressed by long-term chilling does not affect the activities of photosystem 1 or 2. *J Plant Growth Regul* 29:500–505. <https://doi.org/10.1007/s0034-010-9153-0>
- Houimli SIM, Denden M, El Hadj SB (2008) Induction of salt tolerance in pepper (*Capsicum annum*) by 24-epibrassinolide. *Eur Asian J Biosci* 2:83–90
- Houimli SIM, Denden M, Mouhades BD (2010) Effects of 24-epibrassinolide on growth, chlorophyll, electrolyte leakage and proline by pepper plants under NaCl-stress. *Eur Asian J Biosci* 4:96–104. <https://doi.org/10.5053/ejobios.2010.4.0.12>
- IBA (2017) Report 2017: base year 2016. Brasília
- Jesus LR, Batista BL, Lobato AKS (2017) Silicon reduces aluminum accumulation and mitigates toxic effects in cowpea plants. *Acta Physiol Plant* 39:138. <https://doi.org/10.1007/s11738-017-2435-4>

- Kong J, Dong Y, Song Y et al (2015) Role of exogenous nitric oxide in alleviating iron deficiency stress of peanut seedlings (*Arachis hypogaea* L.). *J Plant Growth Regul* 35:31–43. <https://doi.org/10.1007/s00344-015-9504-y>
- Kraemer SM (2004) Iron oxide dissolution and solubility in the presence of siderophores. *Aquat Sci* 66:3–18. <https://doi.org/10.1007/s00027-003-0690-5>
- Krohling CA, Eutrópico FJ, Bertolazi AA et al (2016) Ecophysiology of iron homeostasis in plants. *Soil Sci Plant Nutr* 62:39–47. <https://doi.org/10.1080/00380768.2015.1123116>
- Kumari J, Udawat P, Dubey AK et al (2017) Overexpression of SbSI-1, a nuclear protein from *Salicornia brachiata* confers drought and salt stress tolerance and maintains photosynthetic efficiency in transgenic tobacco. *Front Plant Sci* 8:1215. <https://doi.org/10.3389/fpls.2017.01215>
- Kurusu G, Zhang H, Smith JL, Cramer WA (2002) Structure of the cytochrome b6f complex of oxygenic photosynthesis: tuning the cavity. *Science* 302:1009–1014. <https://doi.org/10.1126/science.1090165>
- Layer G, Reichelt J, Jahn D, Heinz DW (2010) Structure and function of enzymes in heme biosynthesis. *Protein Sci* 19:1137–1161. <https://doi.org/10.1002/pro.405>
- Li YH, Liu YJ, Xu XL et al (2012) Effect of 24-epibrassinolide on drought stress-induced changes in *Chorisporea bungeana*. *Biol Plant* 56:192–196. <https://doi.org/10.1007/s10535-012-0041-2>
- Lichtenthaler HK, Buschmann C (2001) Chlorophylls and carotenoids: measurement and characterization by UV-VIS spectroscopy. In: *Current protocols in food analytical chemistry*. Wiley, Hoboken, pp 431–438
- Lima JV, Lobato AKS (2017) Brassinosteroids improve photosystem II efficiency, gas exchange, antioxidant enzymes and growth of cowpea plants exposed to water deficit. *Physiol Mol Biol Plants* 23:59–72. <https://doi.org/10.1007/s12298-016-0410-y>
- Ma CC, Gao YB, Guo HY, Wang JL (2004) Photosynthesis, transpiration, and water use efficiency of *Caragana microphylla*, *C. intermedia*, and *C. korshinskii*. *Photosynthetica* 42:65–70. <https://doi.org/10.1023/B:PHOT.0000040571.63254.c2>
- Merchant SS, Helmann JD (2012) Elemental economy: microbial strategies for optimizing growth in the face of nutrient limitation. *Adv Microb Physiol* 60:91–210. <https://doi.org/10.1016/B978-0-12-398264-3.00002-4>
- Mora F, Arriagada O, Ballesta P, Ruiz E (2017) Genetic diversity and population structure of a drought-tolerant species of *Eucalyptus*, using microsatellite markers. *J Plant Biochem Biotechnol* 26:274–281. <https://doi.org/10.1007/s13562-016-0389-z>
- Morales F, Belkhdja R, Abadía A, Abadía J (2000) Photosystem II efficiency and mechanisms of energy dissipation in iron-deficient, field-grown pear trees (*Pyrus communis* L.). *Photosynth Res* 63:9–21. <https://doi.org/10.1023/A:1006389915424>
- Mussig C, Fischer S, Altmann T (2002) Brassinosteroid-regulated gene expression. *Plant Physiol* 129:1241–1251. <https://doi.org/10.1104/pp.011003.1>
- Ogweno JO, Song XS, Shi K et al (2008) Brassinosteroids alleviate heat-induced inhibition of photosynthesis by increasing carboxylation efficiency and enhancing antioxidant systems in *Lycopersicon esculentum*. *J Plant Growth Regul* 27:49–57. <https://doi.org/10.1007/s00344-007-9030-7>
- Robinson NJ, Procter CM, Connolly EL, Guerinot M, Lou (1999) A ferric-chelate reductase for iron uptake from soils. *Nature* 397:694–697. <https://doi.org/10.1038/17800>
- Roncel M, González-Rodríguez AA, Naranjo B et al (2016) Iron deficiency induces a partial inhibition of the photosynthetic electron transport and a high sensitivity to light in the diatom *Phaeodactylum tricornerutum*. *Front Plant Sci* 7:1–14. <https://doi.org/10.3389/fpls.2016.01050>
- Rout GR, Sahoo S (2015) Role of iron in plant growth and metabolism. *Rev Agric Sci* 3:1–24. <https://doi.org/10.7831/ras.3.1>
- Sahrawat KL (2004) Iron toxicity in wetland rice and the role of other nutrients. *J Plant Nutr* 27:1471–1504. <https://doi.org/10.1081/PLN-200025869>
- Santi S, Cesco S, Varanini Z, Pinton R (2005) Two plasma membrane H⁺-ATPase genes are differentially expressed in iron-deficient cucumber plants. *Plant Physiol Biochem* 43:287–292. <https://doi.org/10.1016/j.plaphy.2005.02.007>
- Santos LR, Batista BL, Lobato AKS (2018) Brassinosteroids mitigate cadmium toxicity in cowpea plants. *Photosynthetica* 56:591–605. <https://doi.org/10.1007/s11099-017-0700-9>
- Schwertmann U (1991) Solubility and dissolution of iron oxides. *Plant Soil* 130:1–25. <https://doi.org/10.1007/BF00011851>
- Shahbaz M, Ashraf M (2007) Influence of exogenous application of brassinosteroid on growth and mineral nutrients of wheat (*Triticum aestivum* L.) under saline conditions. *Pakistan J Bot* 39:513–522
- Shahbaz M, Ashraf M, Athar H-U-R (2008) Does exogenous application of 24-epibrassinolide ameliorate salt induced growth inhibition in wheat (*Triticum aestivum* L.)? *Plant Growth Regul* 55:51–64. <https://doi.org/10.1007/s10725-008-9262-y>
- Sharma P, Bhardwaj R (2007) Effects of 24-epibrassinolide on growth and metal uptake in *Brassica juncea* L. under copper metal stress. *Acta Physiol Plant* 29:259–263. <https://doi.org/10.1007/s11738-007-0032-7>
- Sharma KM, Sharma DD, Shukla KB, Upadhyay B (2008) Growth partitioning productivity of wheat as influenced by fertilization and foliar application of bio-regulators. *Indian J Plant Physiol* 13:387–393
- Silva EN, Ribeiro RV, Ferreira-Silva SL et al (2012) Coordinate changes in photosynthesis, sugar accumulation and antioxidative enzymes improve the performance of *Jatropha curcas* plants under drought stress. *Biomass Bioenerg* 45:270–279. <https://doi.org/10.1016/j.biombioe.2012.06.009>
- Song YL, Dong YJ, Tian XY et al (2016) Role of foliar application of 24-epibrassinolide in response of peanut seedlings to iron deficiency. *Biol Plant* 60:329–342. <https://doi.org/10.1007/s10535-016-0596-4>
- Steel RG, Torrie JH, Dickey DA (2006) Principles and procedures of statistics: a biometrical approach, 3rd edn. Academic Internet Publishers, Moorpark
- Stepien P, Johnson GN (2009) Contrasting responses of photosynthesis to salt stress in the Glycophyte *Arabidopsis* and the Halophyte *Thellungiella*: role of the plastid terminal oxidase as an alternative electron sink. *Plant Physiol* 149:1154–1165. <https://doi.org/10.1104/pp.108.132407>
- Swamy KN, Rao SR (2006) Influence of brassinosteroids on rooting and growth of geranium (*Pelargonium* sp.) stem cuttings. *Asian J Plant Sci* 5:619–622. <https://doi.org/10.3923/ajps.2006.619.622>
- Swamy KN, Rao SSR (2009) Effect of 24-epibrassinolide on growth, photosynthesis, and essential oil content of *Pelargonium graveolens* (L.) Herit. *Russ J Plant Physiol* 56:616–620. <https://doi.org/10.1134/S1021443709050057>
- Talaat NB, Abdallah AM (2010) Effect of 28-homobrassinolide and 24-epibrassinolide on the growth, productivity and nutritional value of two faba bean (*Vicia faba* L.) cultivars. *Arch Agron Soil Sci* 56:649–669. <https://doi.org/10.1080/03650340903164249>
- Talaat NB, Shawky BT (2013) 24-Epibrassinolide alleviates salt-induced inhibition of productivity by increasing nutrients and compatible solutes accumulation and enhancing antioxidant system in wheat (*Triticum aestivum* L.). *Acta Physiol Plant* 35:729–740. <https://doi.org/10.1007/s11738-012-1113-9>
- Thussaganpanit J, Jutamanee K, Sonjaroon W et al (2015) Effects of brassinosteroid and brassinosteroid mimic on photosynthetic

- efficiency and rice yield under heat stress. *Photosynthetica* 53:312–320. <https://doi.org/10.1007/s11099-015-0106-5>
- Tsai HH, Schmidt W (2017) Mobilization of iron by plant-borne coumarins. *Trends Plant Sci* 22:538–548. <https://doi.org/10.1016/j.tplants.2017.03.008>
- Velikova V, Yordanov I, Edreva A (2000) Oxidative stress and some antioxidant systems in acid rain-treated bean plants protective role of exogenous polyamines. *Plant Sci* 151:59–66. [https://doi.org/10.1016/S0168-9452\(99\)00197-1](https://doi.org/10.1016/S0168-9452(99)00197-1)
- Verma L, Pandey N (2016) Effect of iron stress on oxidative metabolism in wheat plants (*Triticum aestivum* (L.)): iron stress in wheat. *Int J Appl Pure Sci Agric* 2:24–32
- Vert G, Grotz N, Dédaldéchamp F et al (2002) IRT1, an arabidopsis transporter essential for iron uptake from the soil and for plant growth. *Plant Cell* 14:1223–1233. <https://doi.org/10.1105/tpc.001388>
- Wang B, Li Y, Zhang WH (2012) Brassinosteroids are involved in response of cucumber (*Cucumis sativus*) to iron deficiency. *Ann Bot* 110:681–688. <https://doi.org/10.1093/aob/mcs126>
- Wang B, Li G, Zhang WH (2015) Brassinosteroids are involved in Fe homeostasis in rice (*Oryza sativa* L.). *J Exp Bot* 66:2749–2761. <https://doi.org/10.1093/jxb/erv079>
- Wu Q-S, Xia R-X, Zou Y-N (2006) Reactive oxygen metabolism in mycorrhizal and non-mycorrhizal citrus (*Poncirus trifoliata*) seedlings subjected to water stress. *J Plant Physiol* 163:1101–1110. <https://doi.org/10.1016/j.jplph.2005.09.001>
- Xia X-J, Wang Y-J, Zhou Y-H et al (2009) Reactive oxygen species are involved in brassinosteroid-induced stress tolerance in cucumber. *Plant Physiol* 150:801–814. <https://doi.org/10.1104/pp.109.138230>
- Yi Y, Guerinot ML (1996) Genetic evidence that induction of root Fe(III) chelate reductase activity is necessary for iron uptake under iron deficiency. *Plant J* 10:835–844. <https://doi.org/10.1046/j.1365-3113X.1996.10050835.x>
- Yu JQ, Huang LF, Hu WH et al (2004) A role for brassinosteroids in the regulation of photosynthesis in *Cucumis sativus*. *J Exp Bot* 55:1135–1143. <https://doi.org/10.1093/jxb/erh124>
- Yuan L, Shu S, Sun J et al (2012) Effects of 24-epibrassinolide on the photosynthetic characteristics, antioxidant system, and chloroplast ultrastructure in *Cucumis sativus* L. under Ca(NO₃)₂ stress. *Photosynth Res* 112:205–214. <https://doi.org/10.1007/s11120-012-9774-1>
- Yusuf M, Fariduddin Q, Ahmad I, Ahmad A (2014) Brassinosteroid-mediated evaluation of antioxidant system and nitrogen metabolism in two contrasting cultivars of *Vigna radiata* under different levels of nickel. *Physiol Mol Biol Plants* 20:449–460. <https://doi.org/10.1007/s12298-014-0259-x>